# NATIONAL ADVISORY COMMITTEE FOR AERONAUTICS

TECHNICAL NOTE

No. 1633

# AN EVALUATION OF THE CHARACTERISTICS OF A 10-PERCENT-THICK NACA 66-SERIES AIRFOIL SECTION WITH A SPECIAL MEAN-CAMBER LINE DESIGNED TO PRODUCE A HIGH CRITICAL MACH NUMBER

By Laurence K. Loftin, Jr., and Kenneth S. Cohen

Langley Aeronautical Laboratory
Langley Field, Va.

Washington
July 1948

NATIONAL ADVISORY COMMITTEE FOR AERONAUTICS

TECHNICAL NOTE NO. 1633

# AN EVALUATION OF THE CHARACTERISTICS OF A 10-PERCENT-THICK NACA 66-SERIES AIRFOIL SECTION WITH A SPECIAL MEAN-CAMBER LINE DESIGNED TO PRODUCE A HIGH CRITICAL MACH NUMBER

By Laurence K. Loftin, Jr., and Kenneth S. Cohen

## SUMMARY

The low-speed aerodynamic characteristics of the NACA $66_{(09)}$-210 $\begin{Bmatrix} a = 1.0, & c_{l_i} = 0.6 \\ a = 0.6, & c_{l_i} = -0.4 \end{Bmatrix}$ airfoil section were determined from tests in the Langley two-dimensional low-turbulence pressure tunnel. These data and similar data for the NACA 66-210,a=1.0 airfoil are presented. By the use of these low-speed data and high-speed data obtained in the Ames 1- by $3\frac{1}{2}$-foot high-speed tunnel, a comparison of the NACA $66_{(09)}$-210 $\begin{Bmatrix} a = 1.0, & c_{l_i} = 0.6 \\ a = 0.6, & c_{l_i} = -0.4 \end{Bmatrix}$ and NACA 66-210,a=1.0 airfoils was made at both low and high speeds. The high-speed data indicated that the airfoil with the special mean line had a drag-divergence Mach number at the design lift coefficient slightly higher than that of the NACA 66-210,a=1.0 airfoil section, but this increase was not so great as that shown by calculations based on low-speed data of the critical Mach numbers for the two airfoils. With the exception of a negative increase of about 50 percent in the pitching moment, the low-speed characteristics of the airfoil with the special mean line were in essential agreement with those of the same airfoil having the $a = 1.0$ mean line.

## INTRODUCTION

The mean-camber line of an airfoil may be so designed that the induced velocities resulting from the camber will occur over that part of the airfoil chord along which the induced velocities resulting from the basic thickness form are small. Thus, by a proper combination of mean line and basic thickness form, the critical Mach number of a cambered airfoil may be increased above that usually predicted for an airfoil cambered with a more conventional-type mean line such as the $a = 1.0$.

Low-speed tests have been made (reference 1) of a number of 16-percent-thick NACA 66-series basic thickness forms cambered with various types of mean line designed especially to minimize the reduction in critical speed caused by camber.

In order that comprehensive data might be available for such a special airfoil of a thickness more useful for high-speed aircraft, low-speed tests in the Langley two-dimensional low-turbulence pressure tunnel and high-speed tests in the Ames 1- by $3\frac{1}{2}$-foot high-speed tunnel (reference 2) were made of a 10-percent-thick airfoil having a special mean line. The results of the low-speed tests, which included pressure-distribution measurements at a Reynolds number of $6.0 \times 10^6$ and determination of the aerodynamic characteristics of the airfoil at Reynolds numbers of $3.0 \times 10^6$, $6.0 \times 10^6$, and $9.0 \times 10^6$, are presented and analyzed in the present paper. As an aid to the proper interpretation of the critical Mach number data predicted from the low-speed theoretical and experimental pressure distributions, the results of the high-speed tests presented in reference 2 are used.

## COEFFICIENTS AND SYMBOLS

$c_d$ section drag coefficient

$c_l$ section lift coefficient

$c_{l_i}$ design section lift coefficient

$c_{m_{c/4}}$ section quarter-chord pitching-moment coefficient

$c_{m_{ac}}$ section pitching-moment coefficient about aerodynamic center

$\alpha_o$ section angle of attack

$H_o$ free-stream total pressure

$p$ local static pressure

$q_o$ free-stream dynamic pressure

$S$ pressure coefficient $\left(\frac{H_o - p}{q_o}\right)$

$P_R$ resultant pressure coefficient, that is, difference between local upper-surface and lower-surface pressure coefficients

M Mach number

R Reynolds number

a mean-line designation, fraction of chord from leading edge over which design load is uniform

c airfoil chord length

x distance along chord from leading edge

y distance perpendicular to chord

## DESCRIPTION OF AIRFOIL

The airfoil section consisted of an NACA $66_{(09)}$-010 basic thickness distribution combined with a special mean line formed by the superposition of the $a = 1.0$, $c_{l_i} = 0.6$ and the $a = 0.6$, $c_{l_i} = -0.4$ mean lines (references 1 and 3). The load distributions of the two component mean lines together with the distribution for the final mean line resulting from the superposition of the two mean lines are shown in figure 1. The design lift coefficient of the final mean line is 0.2. The composite mean line has linearly increasing induced velocities from 0.6c to the trailing edge, and the NACA 66-series basic thickness form has linearly decreasing induced velocities from 0.6c to the trailing edge. The pressure distribution of the airfoil formed by cambering the NACA 66-series basic thickness form with the special mean line has a maximum negative pressure coefficient higher than that of the basic thickness form at zero lift but less than that of the same basic thickness form cambered with the $a = 1.0$ mean line (fig. 2). A higher critical Mach number at the design lift coefficient is therefore indicated for the airfoil with the special mean line. The ordinates of the cambered airfoil, which is designated NACA $66_{(09)}$-210 $\begin{cases} a = 1.0, & c_{l_i} = 0.6 \\ a = 0.6, & c_{l_i} = -0.4 \end{cases}$, are presented in table I and a sketch of the airfoil is included in figure 3.

## MODEL AND TESTS

The airfoil section was represented by a 24-inch-chord wooden model, the surfaces of which were painted and then sanded until aerodynamically smooth. The tests were made in the Langley two-dimensional low-turbulence pressure tunnel. The test section of this tunnel measures 3 by 7.5 feet with the model, when mounted, completely spanning the 3-foot dimension and with the ends of the model sealed against the tunnel walls to prevent air leakage.

Lift was measured by taking the difference betweeen the pressure reaction upon the floor and ceiling of the tunnel; drag was determined by the wake-survey method; and pitching moments were measured by a torque balance. Measurements of the pressure distribution about the airfoil were made by means of small pressure orifices located on the upper and lower surfaces of the model midway between the vertical walls of the tunnel. A more complete description of the tunnel and the methods of obtaining and reducing the data are contained in reference 4.

Lift, drag, and pitching-moment measurements were made for the plain airfoil in the smooth condition at Reynolds numbers of $3.0 \times 10^6$, $6.0 \times 10^6$, and $9.0 \times 10^6$. The lift and moment characteristics of the airfoil equipped with a simulated split flap deflected $60^\circ$ were measured at a Reynolds number of $6.0 \times 10^6$. In order to show the effect of surface condition upon the aerodynamic characteristics, lift and drag tests of the airfoil were made with standard roughness applied to the leading edge of the model. The roughness employed on the 24-inch-chord model consisted of 0.011-inch-diameter carborundum grains spread over a surface length of $0.08c$ behind the leading edge of the airfoil on the upper and lower surfaces. The grains were thinly spread to cover from 5 to 10 percent of this area. The pressure distributions corresponding to a range of angle of attack extending from the positive to the negative stall were determined for the smooth plain airfoil at a Reynolds number of $6.0 \times 10^6$.

## RESULTS AND DISCUSSION

The influence of the tunnel boundaries has been removed from all the aerodynamic data by means of the following relations (developed in reference 4):

$$c_l = 0.974 c_l'$$

$$\alpha_o = 1.015 \alpha_o'$$

$$c_{m_{c/4}} = 0.989 c_{m_{c/4}}'$$

$$c_d = 0.989 c_d'$$

where the primed quantities represent the measured coefficients. The corrections made to the pressure data were derived on the same basis and were of the same order of magnitude as those made to the coefficients.

Critical-speed characteristics.- The critical-speed data predicted from theoretical low-speed pressure distributions by the method of reference 5 indicate that the airfoil with the special mean line has critical Mach numbers which are about 0.015 larger than those of the same airfoil with the $a = 1.0$ mean line (fig. 4). This increase is only apparent within that range of lift coefficient over which the critical Mach number varies linearly.

The center of that range of lift coefficient within which the critical Mach number varies linearly with lift coefficient changes to a value less than the theoretical design lift coefficient when the experimental rather than the theoretical low-speed pressure distributions are used for predicting the critical Mach numbers (fig. 4). The term "effective design lift coefficient" is used when referring to this experimental center. A decrease in the extent of the high critical Mach number range and an increase in the values of the critical Mach numbers within this range are also evident when the critical-speed curve predicted from the experimental pressure distribution is compared with that predicted from the theoretical pressure distributions. These same trends are noted in the results for some of the airfoils discussed in reference 1.

Some insight into the differences between the critical-speed characteristics of the airfoil as predicted from theoretical and experimental low-speed pressure distributions may be gained from figure 5. Shown in figure 5 are data representing the experimental pressure distribution for which the gradients most nearly agree over the forward part of the airfoil with those calculated theoretically for the design-lift condition. The failure of the theoretical load distribution to be realized experimentally for this condition (fig. 5) is responsible for the previously mentioned differences between the theoretical and effective design lift coefficients. A study of figure 6 indicates the formation of negative pressure peaks near the leading edge to be responsible for the short range of lift coefficient through which the critical Mach number varies linearly. The experimental peak negative pressure for the effective design-lift condition is less than that for the theoretical design lift coefficient (fig. 5), which accounts for the difference in magnitude of the critical Mach numbers corresponding to the theoretical and effective design lift coefficients (fig. 4).

The experimental pressure distributions of airfoils with the $a = 1.0$ type mean line agree quite well with those predicted theoretically (reference 3). The critical-speed characteristics of the airfoil with the special mean line, relative to those of the airfoil with the $a = 1.0$ type mean line, would seem therefore to depend upon which type of pressure distribution, theoretical or experimental, is considered as a basis for predicting the critical Mach numbers. Fortunately, in view of the confusing critical-speed results, high-speed data exist (reference 2) which permit an evaluation of the airfoil with the special mean line on the basis of drag-divergence Mach numbers. High-speed data are presented in reference 2 for a special mean-line airfoil similar to the airfoil considered in the present investigation, except that the rear

part of the basic thickness form was thickened to remove the trailing-edge cusp. Included also in reference 2 are high-speed data for the NACA 66-210,a=1.0 airfoil section.

Experimental values of the Mach numbers for drag divergence taken from reference 2 are included in figure 4 for the airfoils with the special mean line and the $a = 1.0$ type mean line. A study of these data show that, for a lift coefficient equal to or greater than the design value, the advantage to be realized experimentally by the use of the airfoil with the special mean line is somewhat less than predicted from theoretical pressure distributions. For lift coefficients less than 0.1, the conventional $a = 1.0$ mean line seems to give better results. The penalty of a reduced range of lift coefficient for high drag-divergence Mach numbers, indicated by the critical-speed data predicted from low-speed experimental pressure distributions, appears - but to a lesser degree - in the drag-divergence data. Perhaps of more significance, however, than the rather small advantage shown by the airfoil with the special mean line is the fact that the range of lift coefficient for high drag-divergence Mach numbers is much greater for both airfoils, and the values of the drag-divergence Mach numbers within this range are higher than indicated by the critical Mach number data predicted from the low-speed pressure distributions.

Low-speed characteristics.- Comparison of the low-speed aerodynamic characteristics of the airfoil having the special mean line (fig. 7) with those taken from reference 3 for the NACA 66-210,a=1.0 airfoil (fig. 8) indicates that, with the exception of a negative increase of approximately 50 percent in the pitching moment, the characteristics of the airfoil with the special mean line are essentially the same as those of the airfoil with the $a = 1.0$ mean line. The failure of the airfoil to realize its theoretical design lift coefficient of 0.2 (fig. 7) is explained by the previously discussed discrepancies in the theoretical and experimental pressure distributions at low speeds.

## CONCLUDING REMARKS

By the use of high-speed aerodynamic data from the Ames 1- by $3\frac{1}{2}$-foot high-speed tunnel and low-speed data from the Langley two-dimensional low-turbulence pressure tunnel, a comparison of the NACA $66_{(09)}$-210 $\begin{Bmatrix} a = 1.0, & c_{l_i} = 0.6 \\ a = 0.6, & c_{l_i} = -0.4 \end{Bmatrix}$ and the NACA 66-210,a=1.0 airfoil sections was made. The high-speed data indicated that the NACA $66_{(09)}$-210 $\begin{Bmatrix} a = 1.0, & c_{l_i} = 0.6 \\ a = 0.6, & c_{l_i} = -0.4 \end{Bmatrix}$ had a drag-divergence Mach number at the design lift coefficient slightly higher than that of the

NACA 66-210,a=1.0, but this increase was not so great as that shown by calculations based on low-speed data of the critical Mach numbers for the two airfoils. With the exception of a negative increase of about 50 percent in the pitching moment, the low-speed characteristics of the NACA $66_{(09)}$-210 $\left\{\begin{matrix} a = 1.0,\ c_{l_i} = 0.6 \\ a = 0.6,\ c_{l_i} = -0.4 \end{matrix}\right\}$ airfoil section were essentially the same as those of the NACA 66-210,a=1.0 airfoil section.

Langley Memorial Aeronautical Laboratory
National Advisory Committee for Aeronautics
Langley Field, Va., February 9, 1948

## REFERENCES

1. von Doenhoff, Albert E., Stivers, Louis S., Jr., and O'Connor, James M.: Low-Speed Tests of Five NACA 66-Series Airfoils having Mean Lines Designed to Give High Critical Mach Numbers. NACA TN No. 1276, 1947.

2. Graham, Donald J.: High-Speed Tests of an Airfoil Section Cambered to Have Critical Mach Numbers Higher Than Those Attainable with a Uniform-Load Mean Line. NACA TN No. 1396, 1947.

3. Abbott, Ira H., von Doenhoff, Albert E., and Stivers, Louis S., Jr.: Summary of Airfoil Data. NACA ACR L5C05, 1945.

4. von Doenhoff, Albert E., and Abbott, Frank T., Jr.: The Langley Two-Dimensional Low-Turbulence Pressure Tunnel. NACA TN No. 1283, 1947.

5. von Kármán, Th.: Compressibility Effects in Aerodynamics. Jour. Aero. Sci., vol. 8, no. 9, July 1941, pp. 337-356.

TABLE I

ORDINATES OF THE

NACA 66(09)-210 $\begin{cases} a = 1.0, & c_{l_i} = 0.6 \\ a = 0.6, & c_{l_i} = -0.4 \end{cases}$

AIRFOIL SECTION

[Stations and ordinates given in percent of airfoil chord]

| Upper surface | | Lower surface | |
|---|---|---|---|
| Station | Ordinate | Station | Ordinate |
| 0 | 0 | 0 | 0 |
| .475 | .783 | .525 | -.743 |
| .722 | .944 | .778 | -.888 |
| 1.220 | 1.187 | 1.280 | -1.101 |
| 2.469 | 1.590 | 2.531 | -1.450 |
| 4.968 | 2.205 | 5.032 | -1.973 |
| 7.469 | 2.687 | 7.531 | -2.387 |
| 9.971 | 3.095 | 10.029 | -2.741 |
| 14.975 | 3.752 | 15.025 | -3.310 |
| 19.979 | 4.251 | 20.021 | -3.751 |
| 24.983 | 4.634 | 25.017 | -4.092 |
| 29.985 | 4.925 | 30.015 | -4.349 |
| 34.986 | 5.135 | 35.014 | -4.527 |
| 39.985 | 5.271 | 40.015 | -4.633 |
| 44.980 | 5.336 | 45.020 | -4.662 |
| 49.971 | 5.333 | 50.029 | -4.611 |
| 54.955 | 5.265 | 55.045 | -4.471 |
| 59.913 | 5.131 | 60.087 | -4.209 |
| 64.886 | 4.891 | 65.114 | -3.731 |
| 69.901 | 4.522 | 70.099 | -3.094 |
| 74.934 | 4.029 | 75.066 | -2.363 |
| 79.973 | 3.425 | 80.027 | -1.603 |
| 85.009 | 2.721 | 84.991 | -.859 |
| 90.030 | 1.917 | 89.970 | -.219 |
| 95.029 | 1.033 | 94.971 | -.203 |
| 100.000 | 0 | 100.000 | 0 |

L.E. radius: 0.643
Slope of radius through L.E.: 0.033

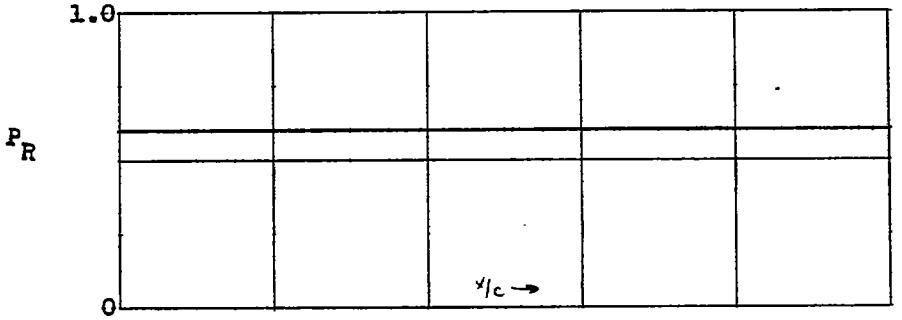


(a) Load distribution of the NACA a = 1.0, $c_{l_i}$ = 0.6 mean line.

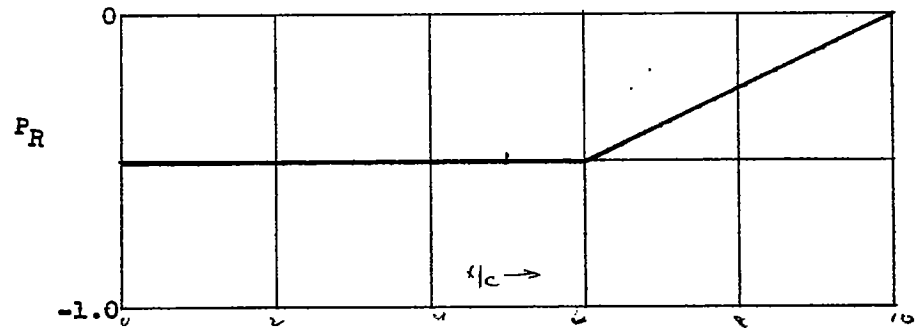


(b) Load distribution of the NACA a = 0.6, $c_{l_i}$ = -0.4 mean line.

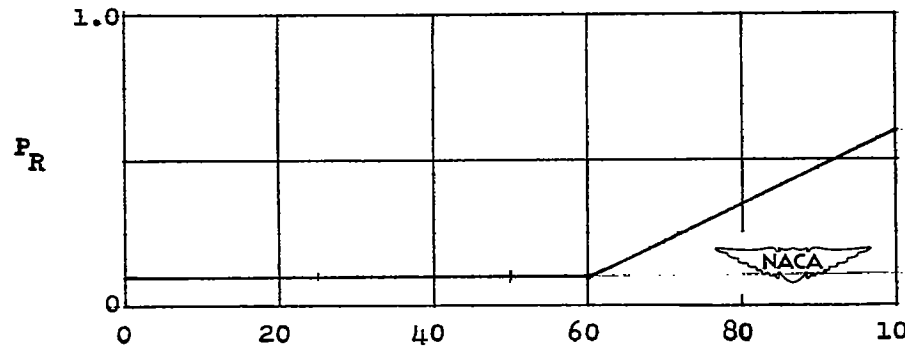


(c) Load distribution of the NACA $\begin{cases} a = 1.0, & c_{l_i} = 0.6 \\ a = 0.6, & c_{l_i} = -0.4 \end{cases}$ mean line (formed by superposition of the load distributions of the NACA a = 1.0, $c_{l_i}$ = 0.6 and NACA a = 0.6, $c_{l_i}$ = -0.4 mean lines).

Figure 1.- Load distribution of the mean line NACA $\begin{cases} a = 1.0, & c_{l_i} = 0.6 \\ a = 0.6, & c_{l_i} = -0.4 \end{cases}$ and component mean lines from which it is formed.

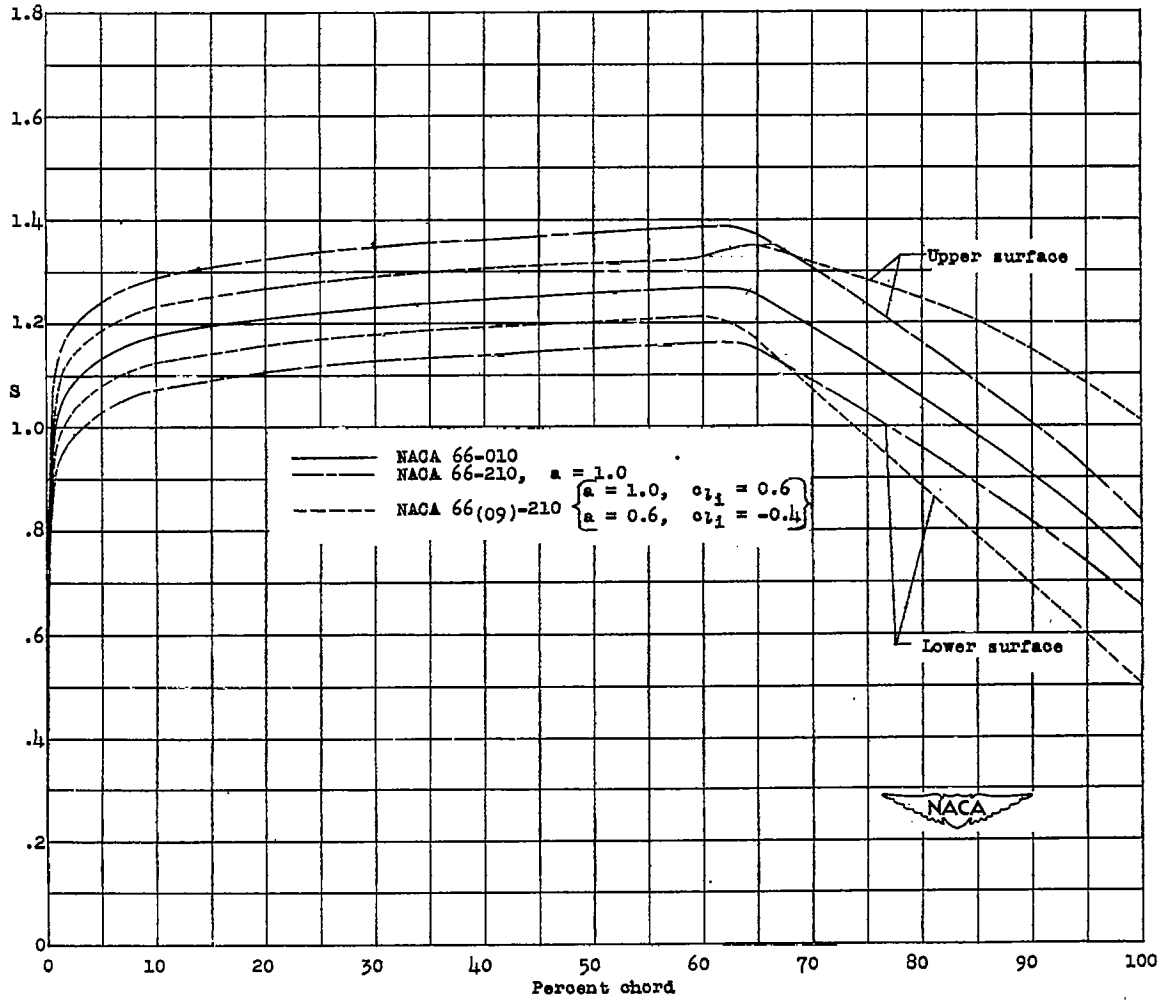


Figure 2.- Comparison of theoretical pressure distributions of several airfoils at their design lift coefficient.

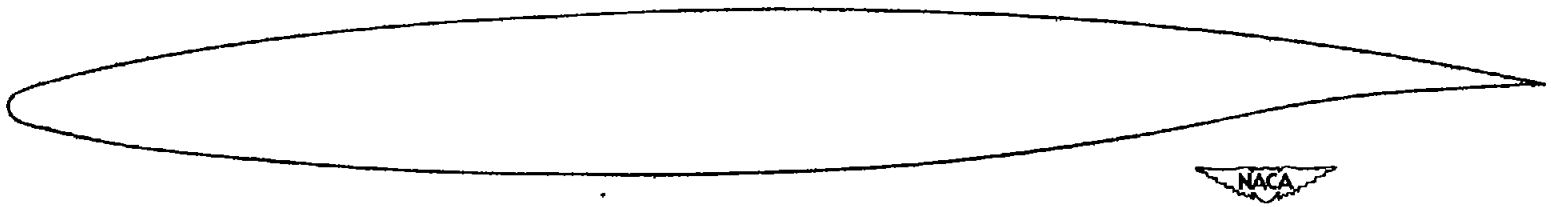

Figure 3.- NACA $66_{(09)}$-210, $\left\{\begin{matrix} a = 1.0, & c_{l_i} = 0.6 \\ a = 0.6, & c_{l_i} = -0.4 \end{matrix}\right\}$ airfoil section.

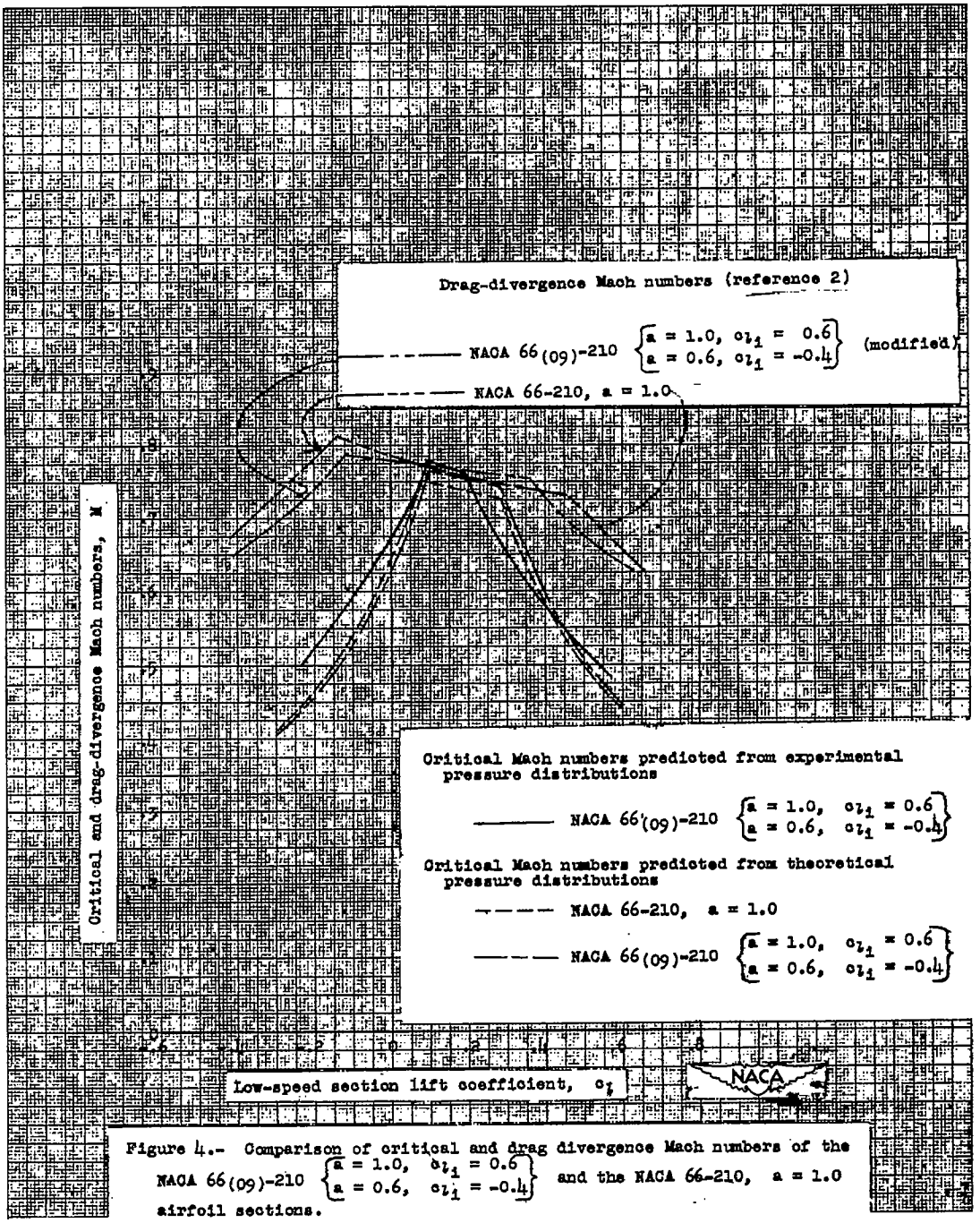


Figure 4.- Comparison of critical and drag divergence Mach numbers of the NACA 66(09)-210 $\begin{cases} a = 1.0, & c_{l_i} = 0.6 \\ a = 0.6, & c_{l_i} = -0.4 \end{cases}$ and the NACA 66-210, a = 1.0 airfoil sections.

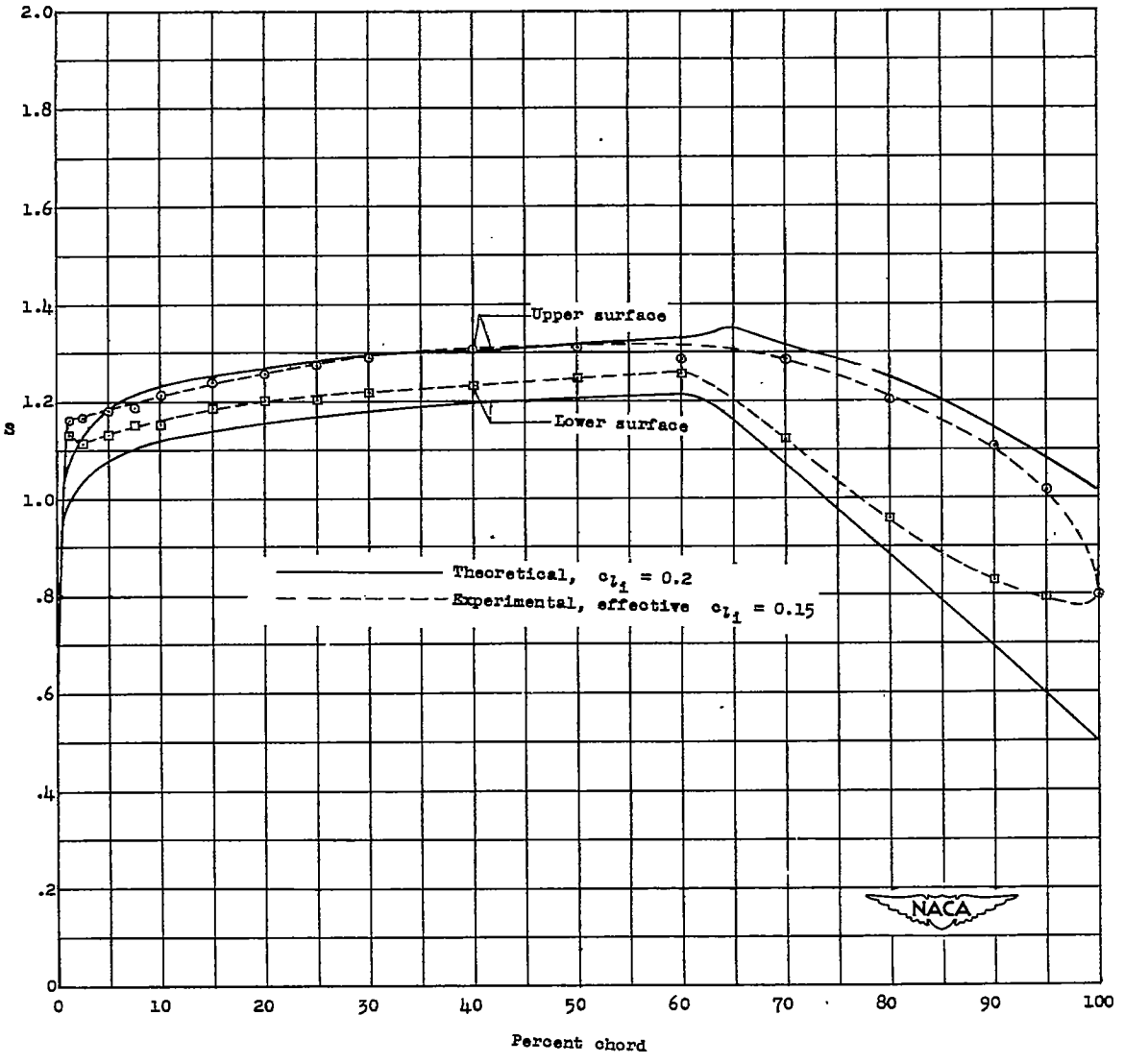


Figure 5.- Comparison of the experimental pressure distribution of the NACA 66(09)-210 $\begin{Bmatrix} a = 1.0, & c_{l_i} = 0.6 \\ a = 0.6, & c_{l_i} = -0.4 \end{Bmatrix}$ airfoil at the effective design lift coefficient with the theoretical pressure distribution at the design lift coefficient.

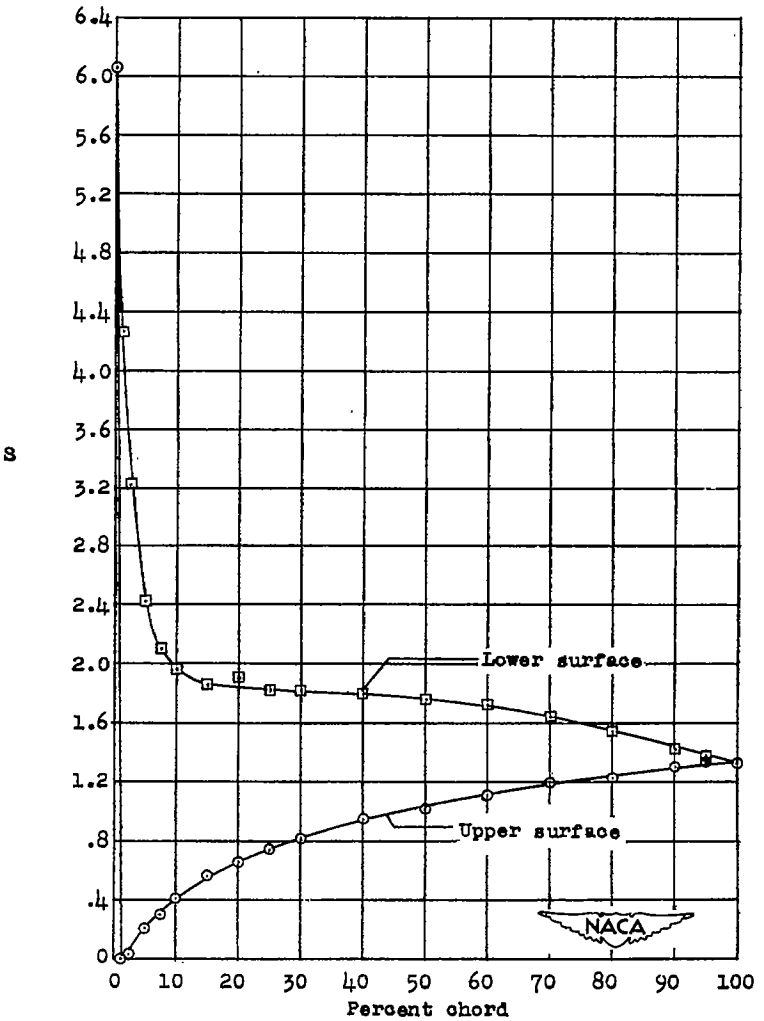


(a) $\alpha_o = -12.0^\circ$; $c_l = -0.65$.

Figure 6.- Experimental pressure distribution of the NACA $66_{(09)}$-210 $\begin{cases} a = 1.0, & c_{l_i} = 0.6 \\ a = 0.6, & c_{l_i} = -0.4 \end{cases}$ airfoil section, $R = 6.0 \times 10^6$.

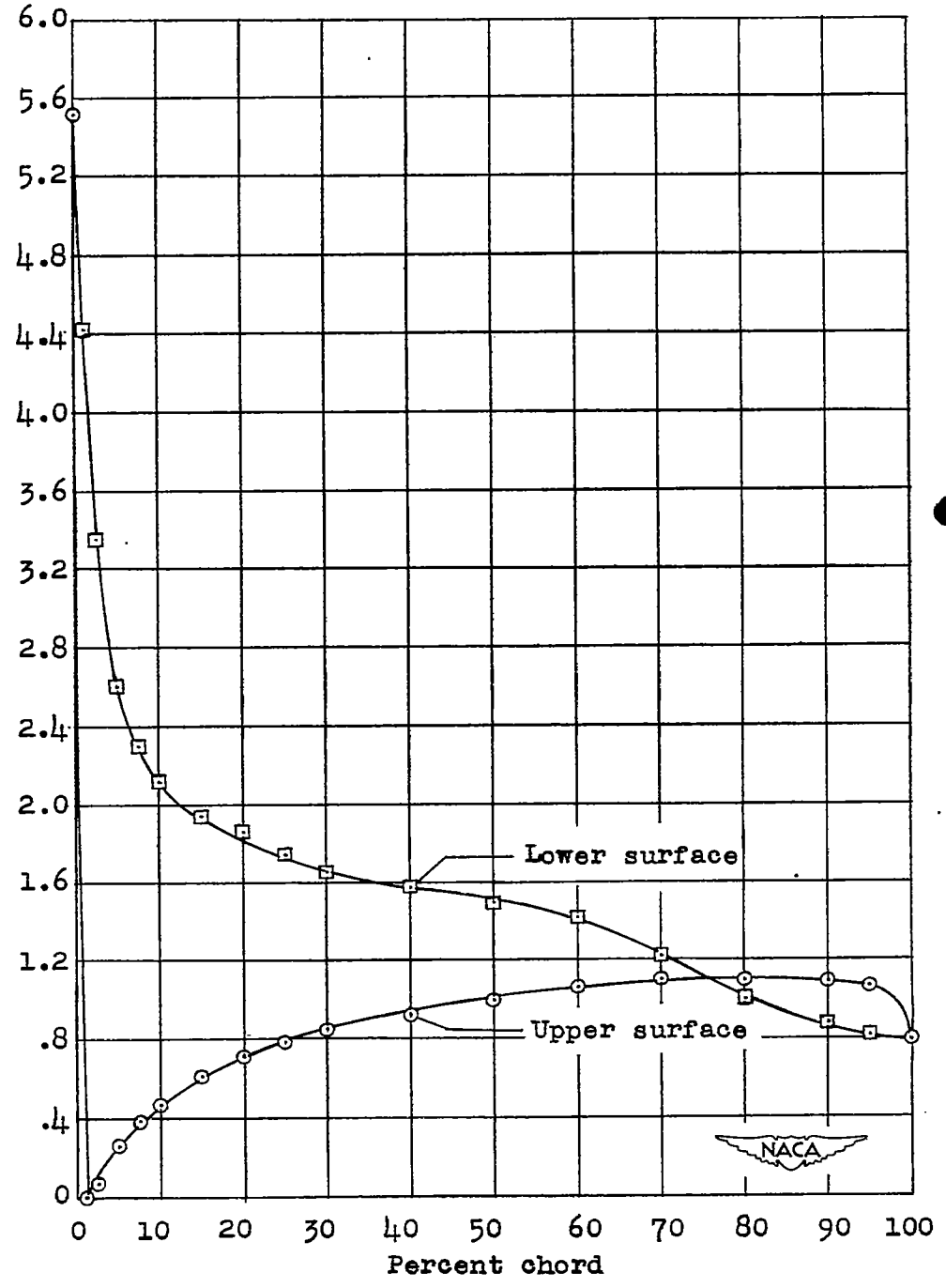


(b) $\alpha_o = -8.0^\circ$; $c_l = -0.55$.

Figure 6.- Continued.

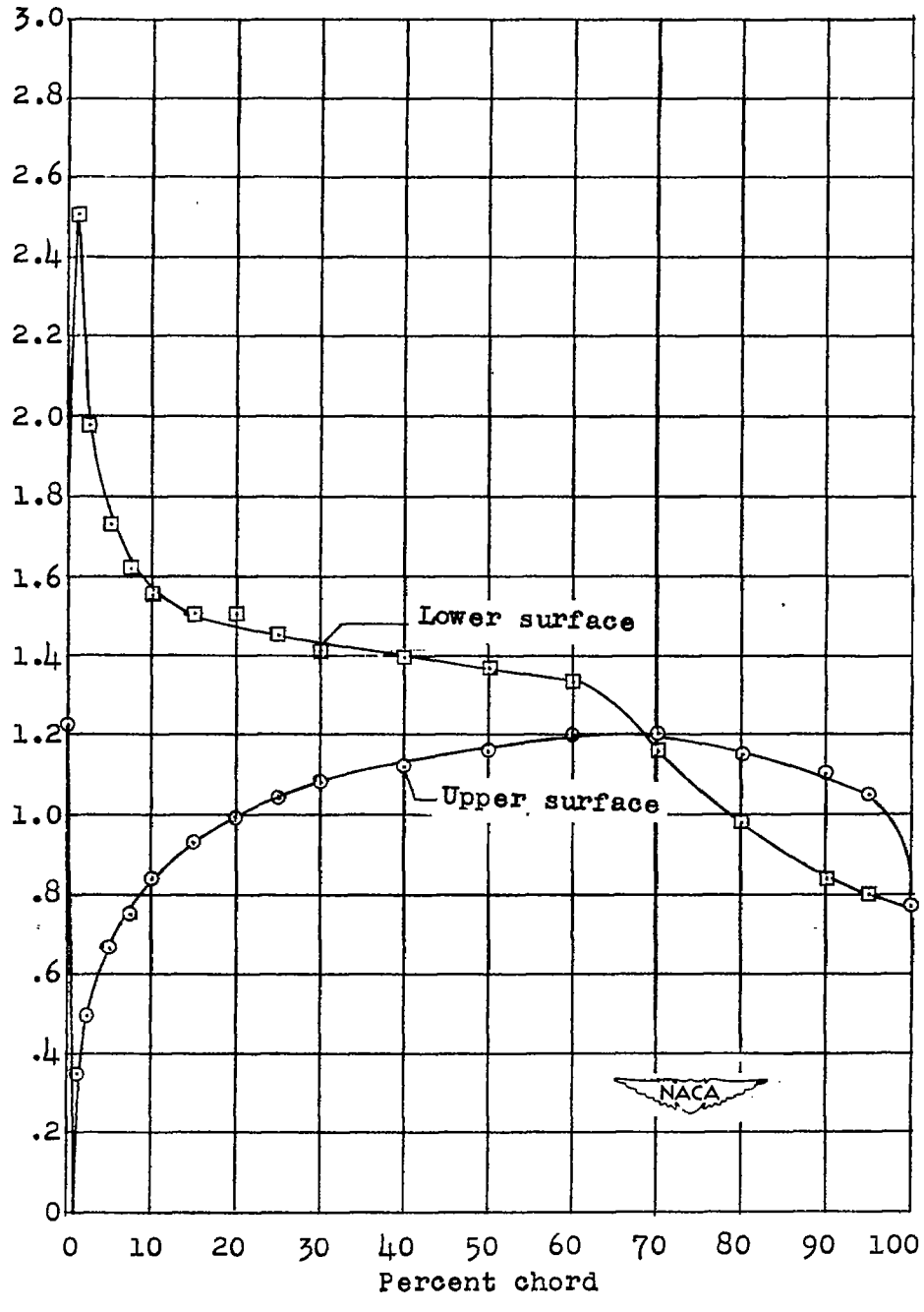


(c) $\alpha_o = -4.0°$; $c_l = -0.24$.

Figure 6.- Continued.

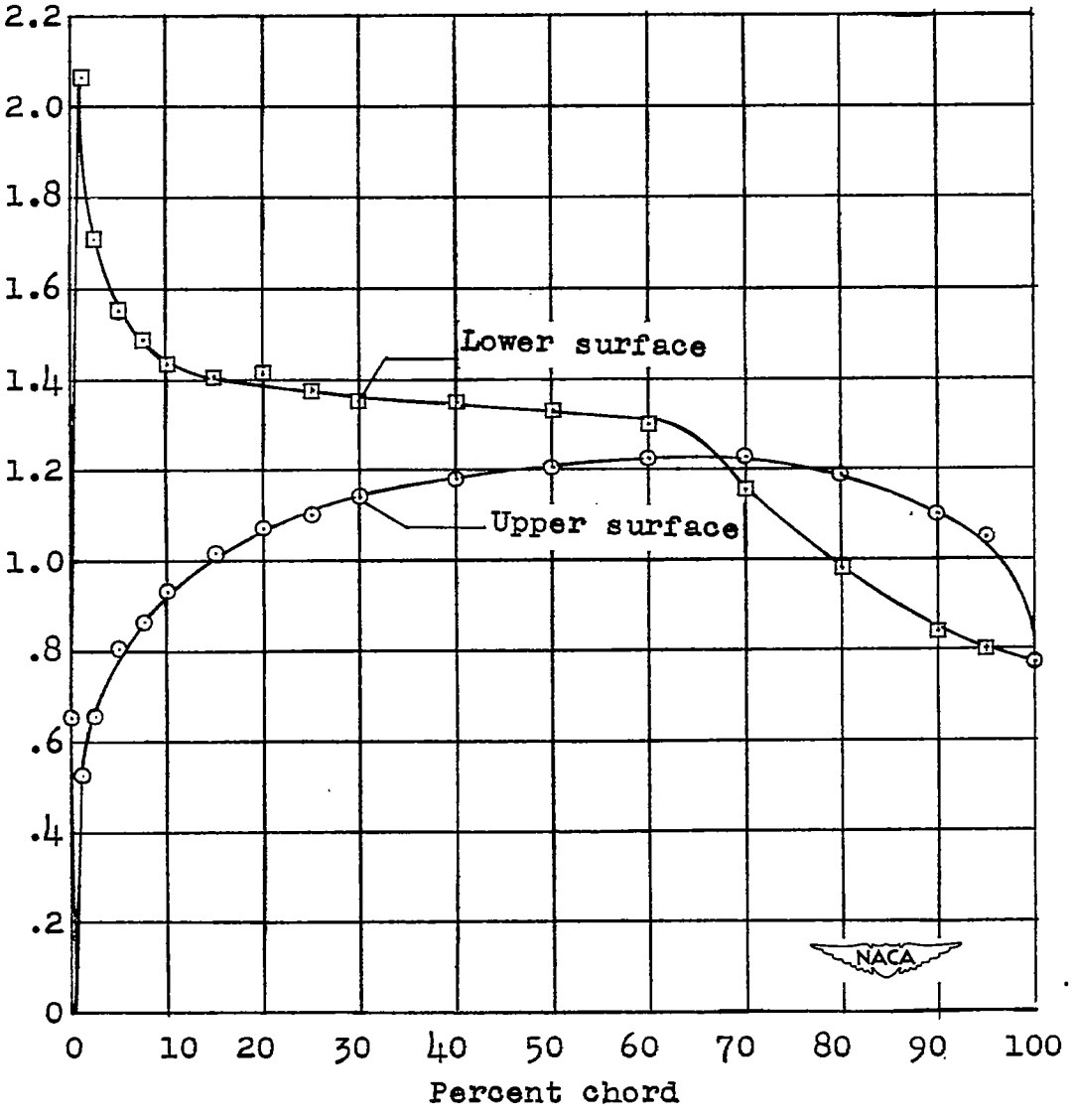


(d) $\alpha_o = -3.0^\circ$; $c_l = -0.13$.

Figure 6.- Continued.

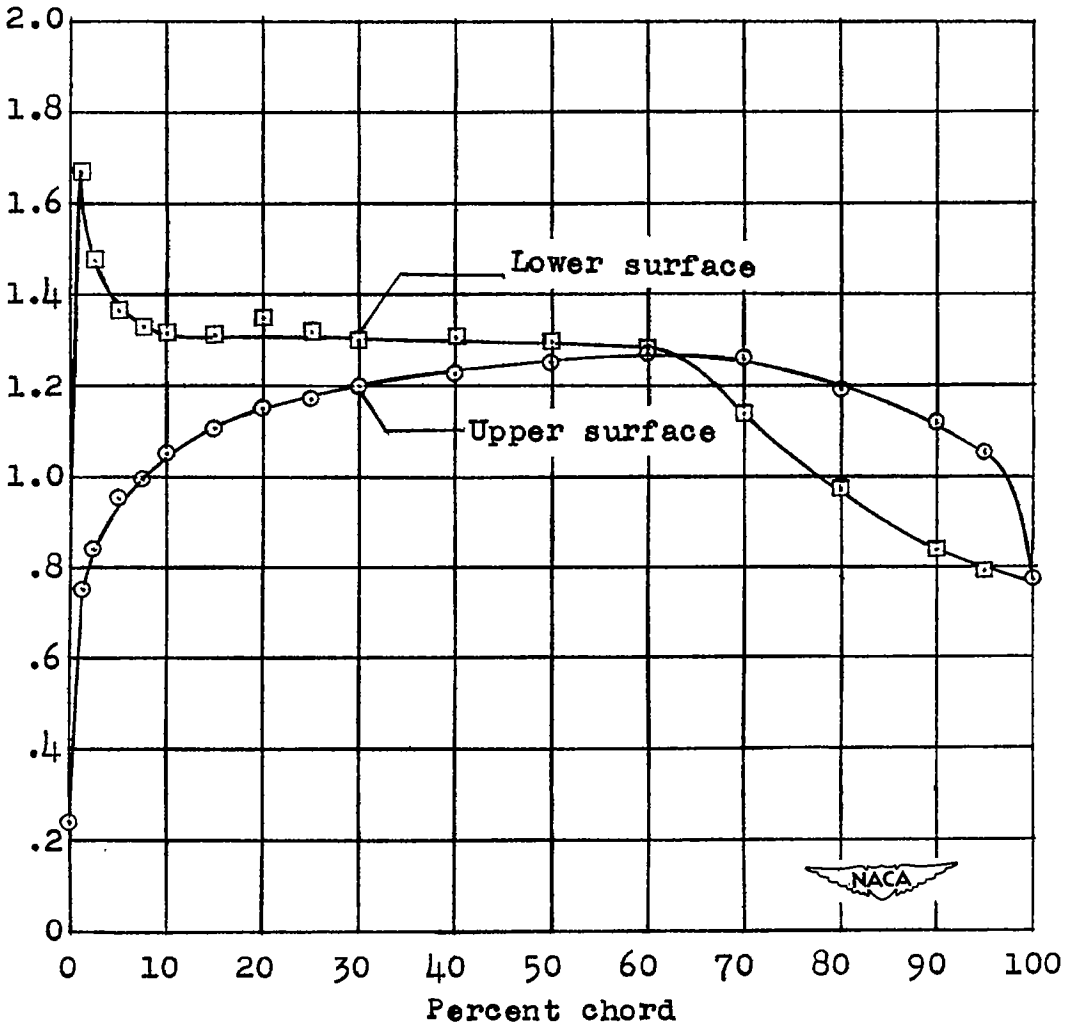


(e) $\alpha_o = -2.0°$; $c_l = 0$.

Figure 6.- Continued.

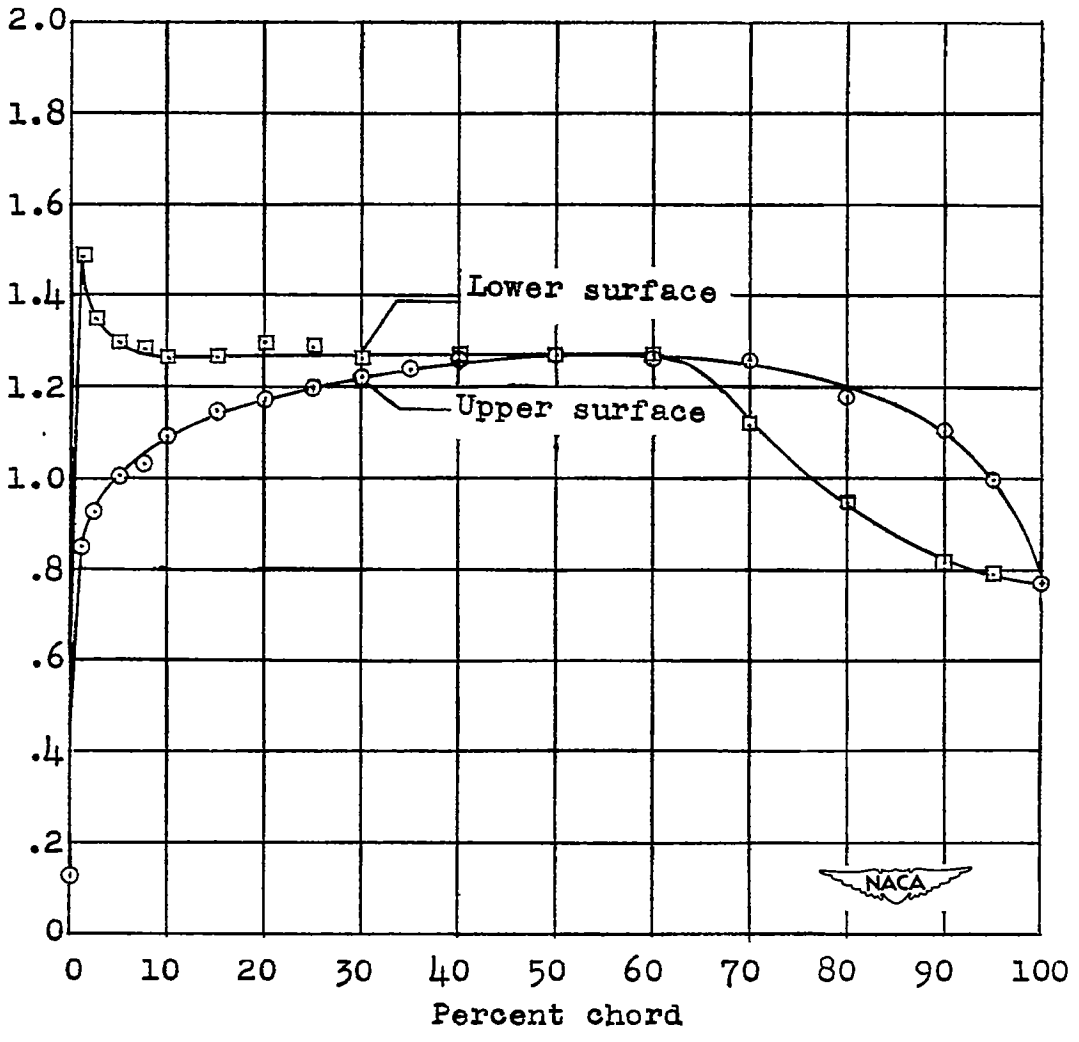


(f) $\alpha_o = -1.5^\circ$; $c_l = 0.03$.

Figure 6.- Continued.

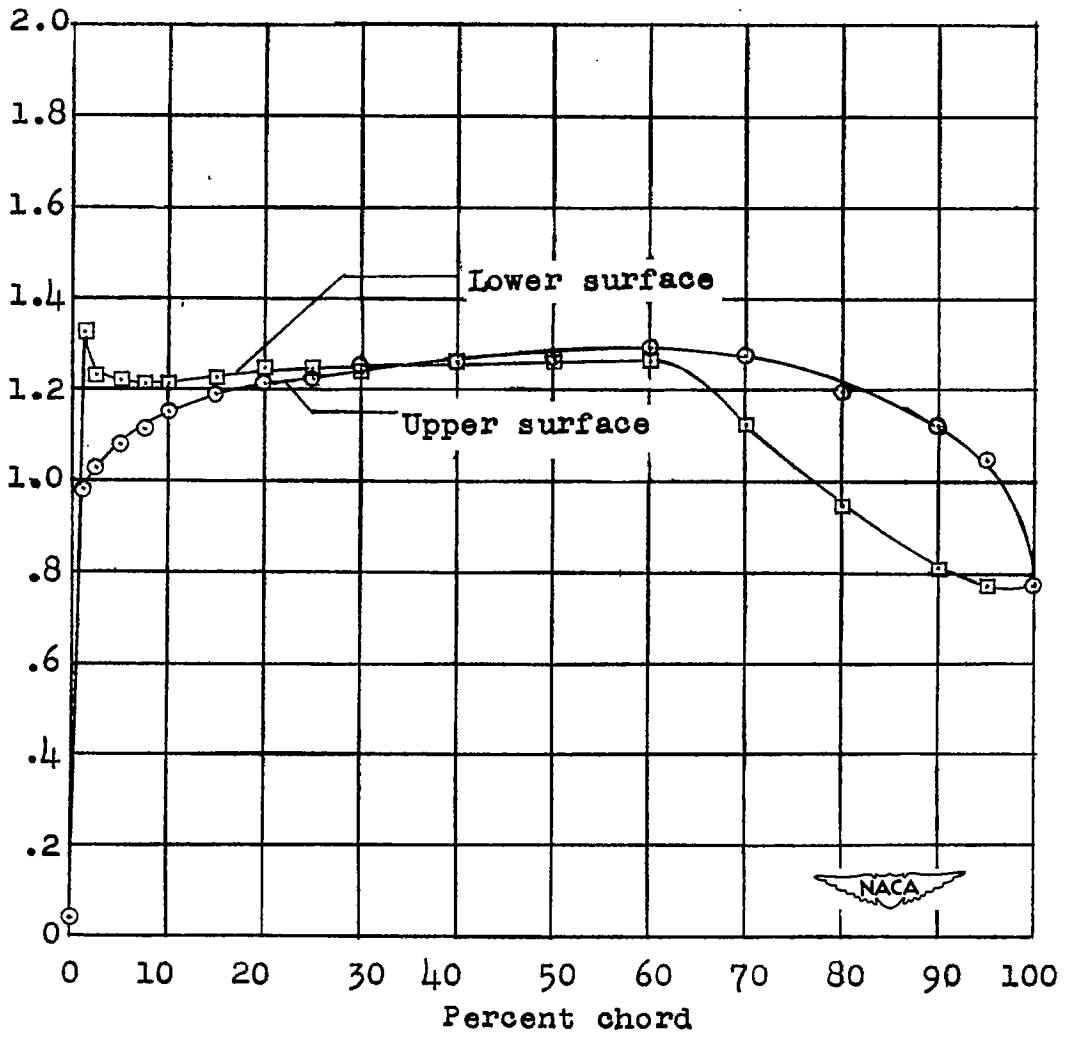


(g) $\alpha_o = -1.0$; $c_l = 0.05$.

Figure 6.- Continued.

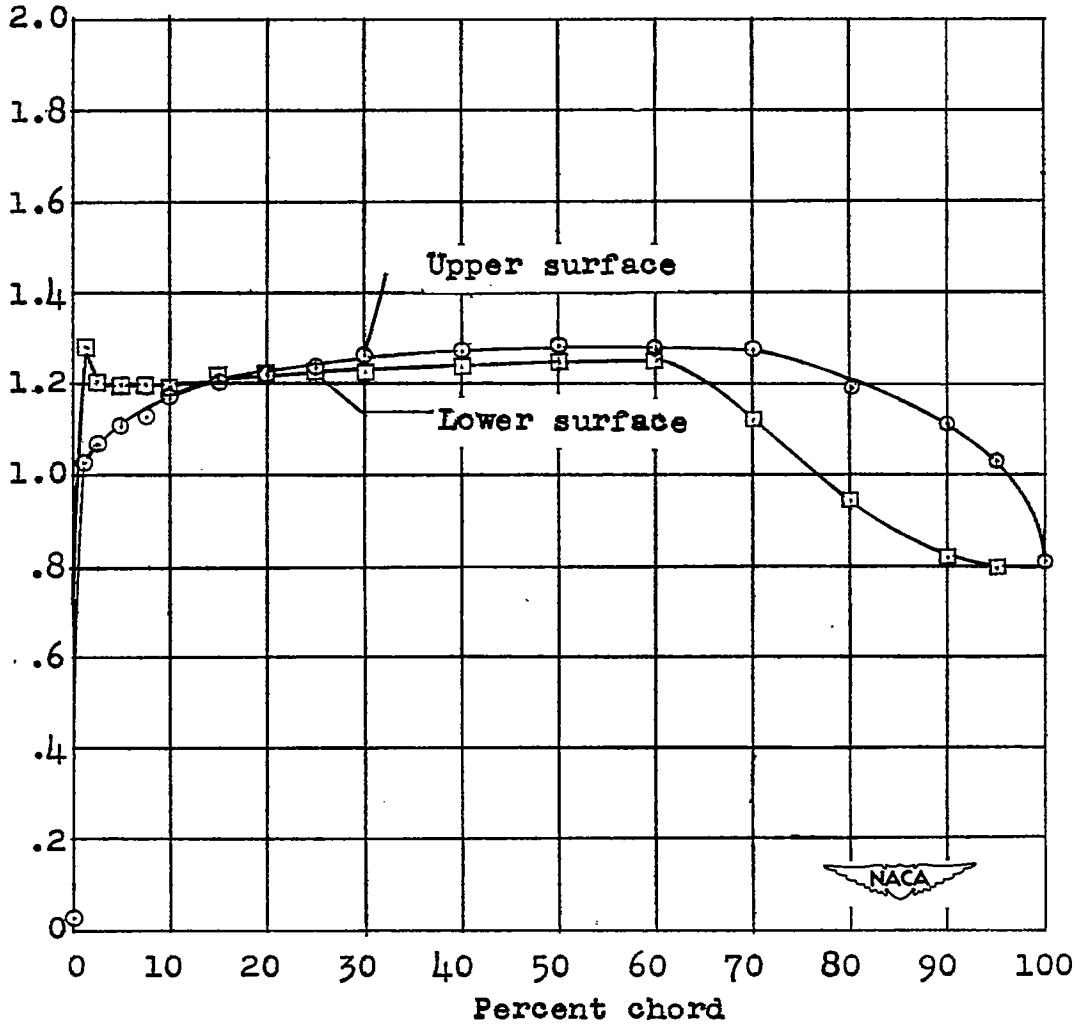


(h) $\alpha_o = -0.8°$; $c_l = 0.08$.

Figure 6.- Continued.

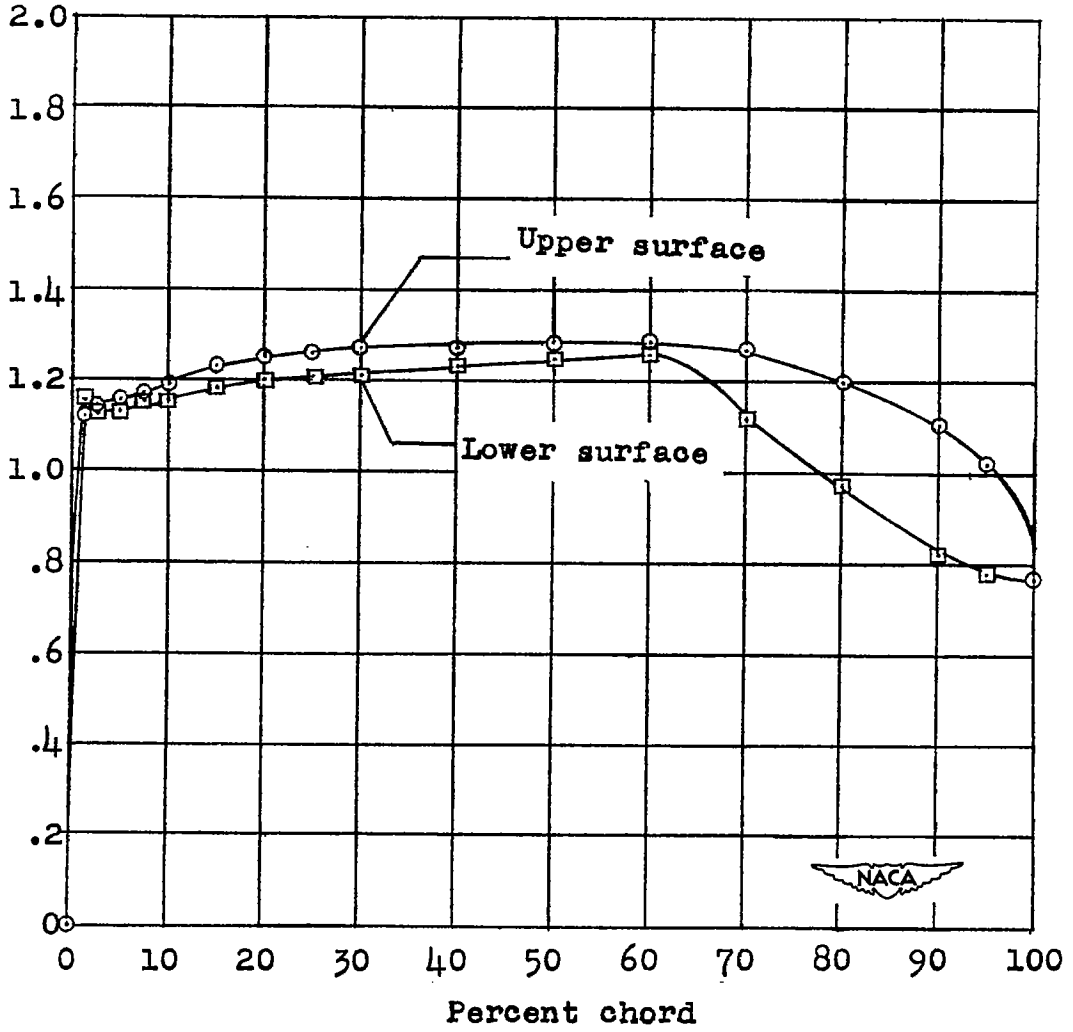


(i) $\alpha_o = -0.5°$; $c_l = 0.10$.

Figure 6.- Continued.

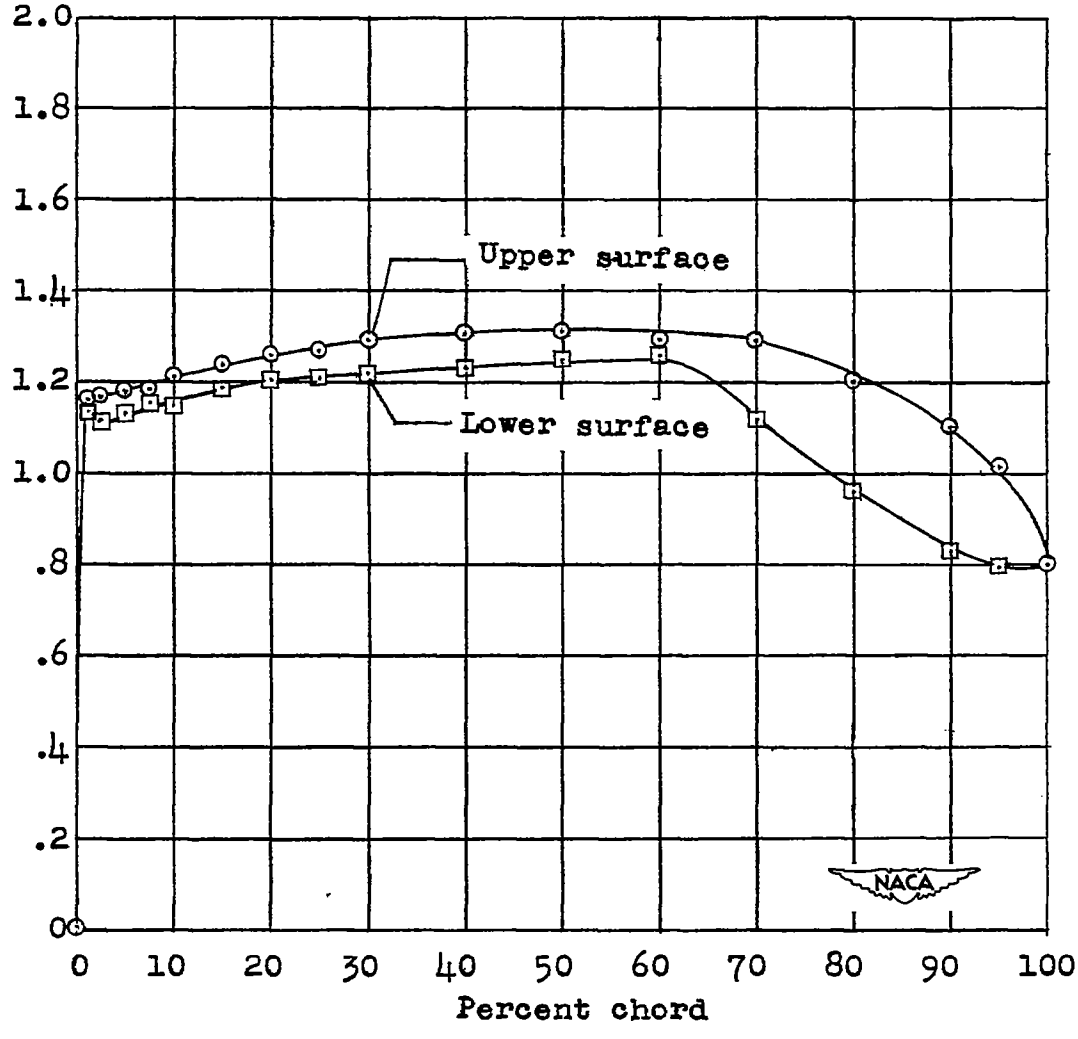


(j) $\alpha_o = -0.3°$; $c_l = 0.15$.

Figure 6.- Continued.

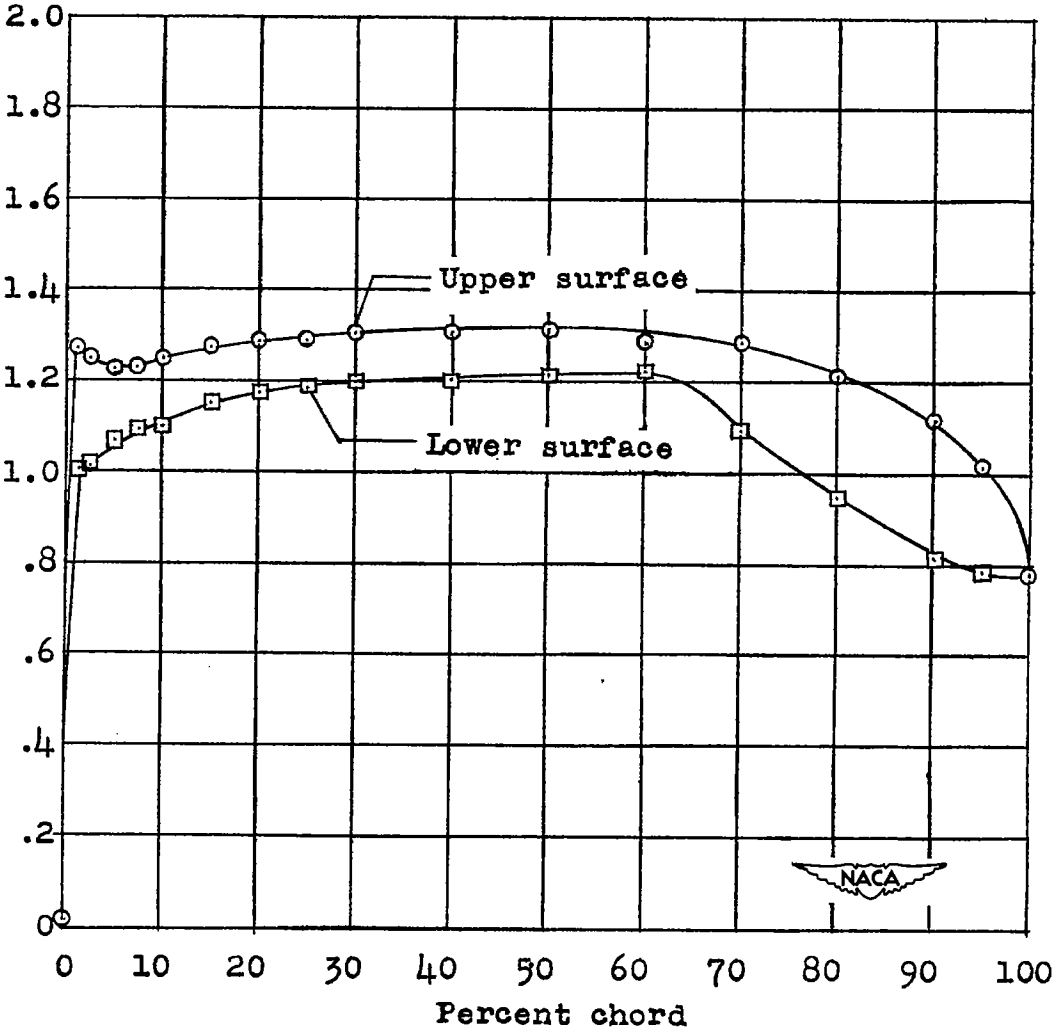


(k) $\alpha_o = 0^\circ$; $c_l = 0.18$.

Figure 6.- Continued.

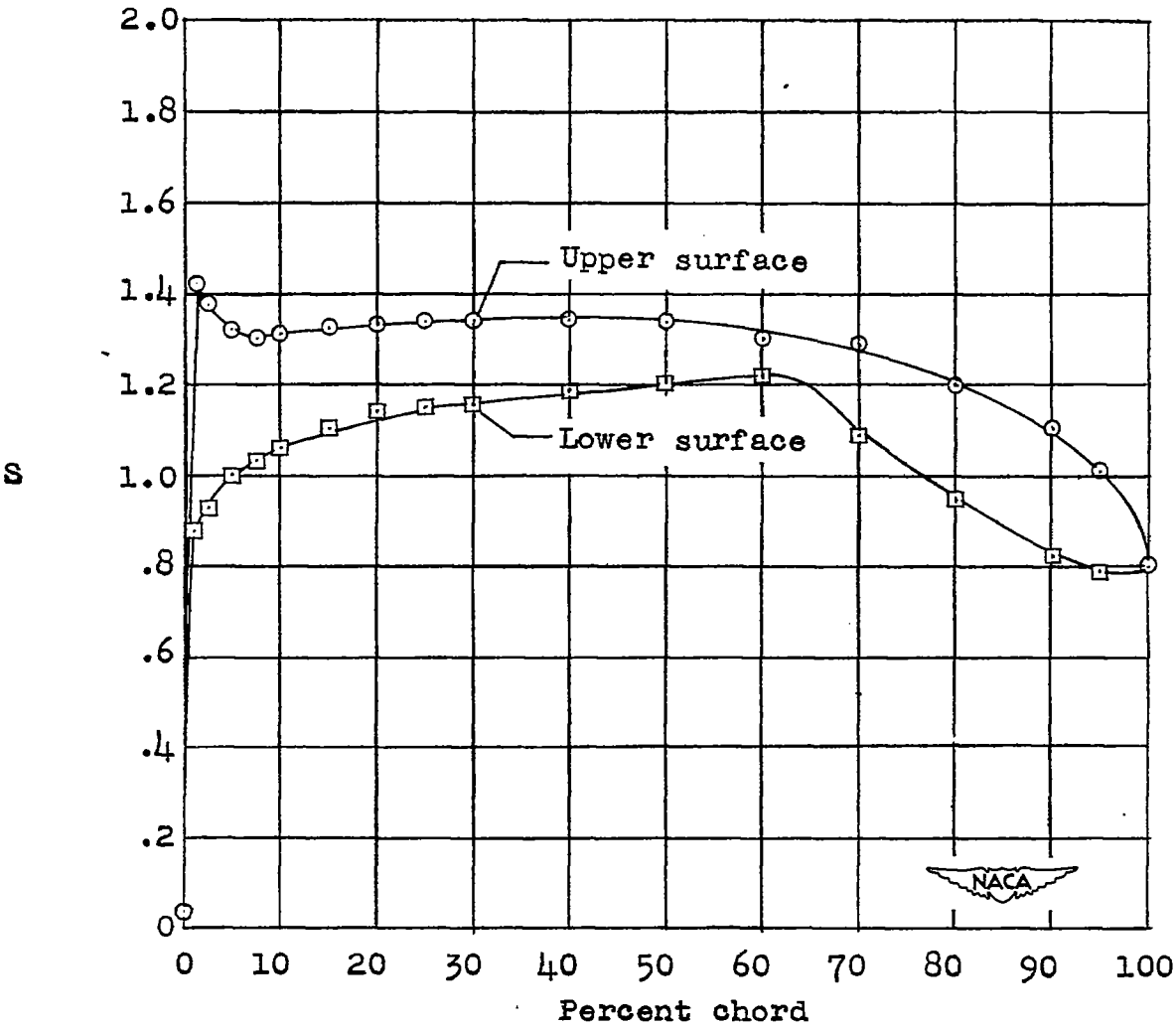


(l) $\alpha_o = 0.5°$; $c_l = 0.23$.

Figure 6.- Continued.

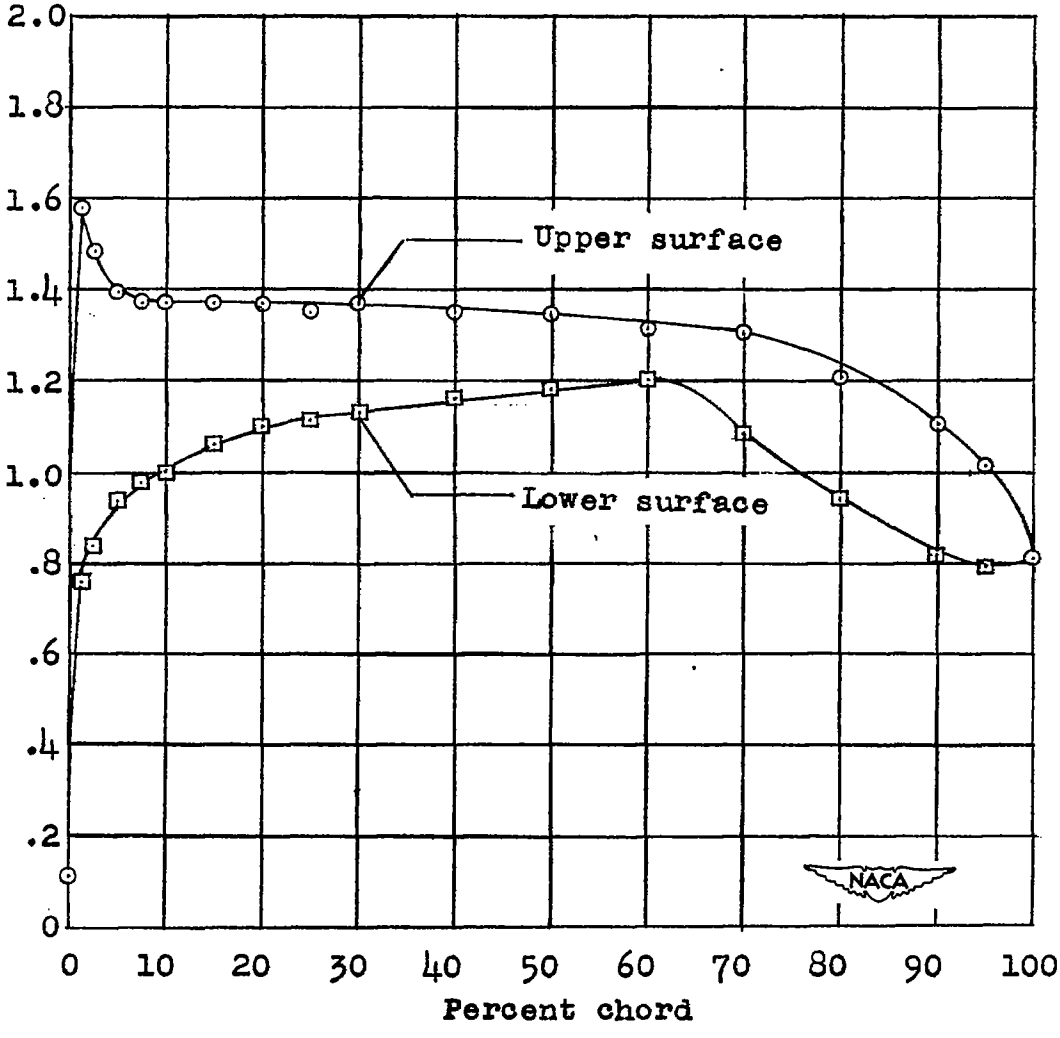


(m) $\alpha_o = 1.0^\circ$; $c_l = 0.27$.

Figure 6.- Continued.

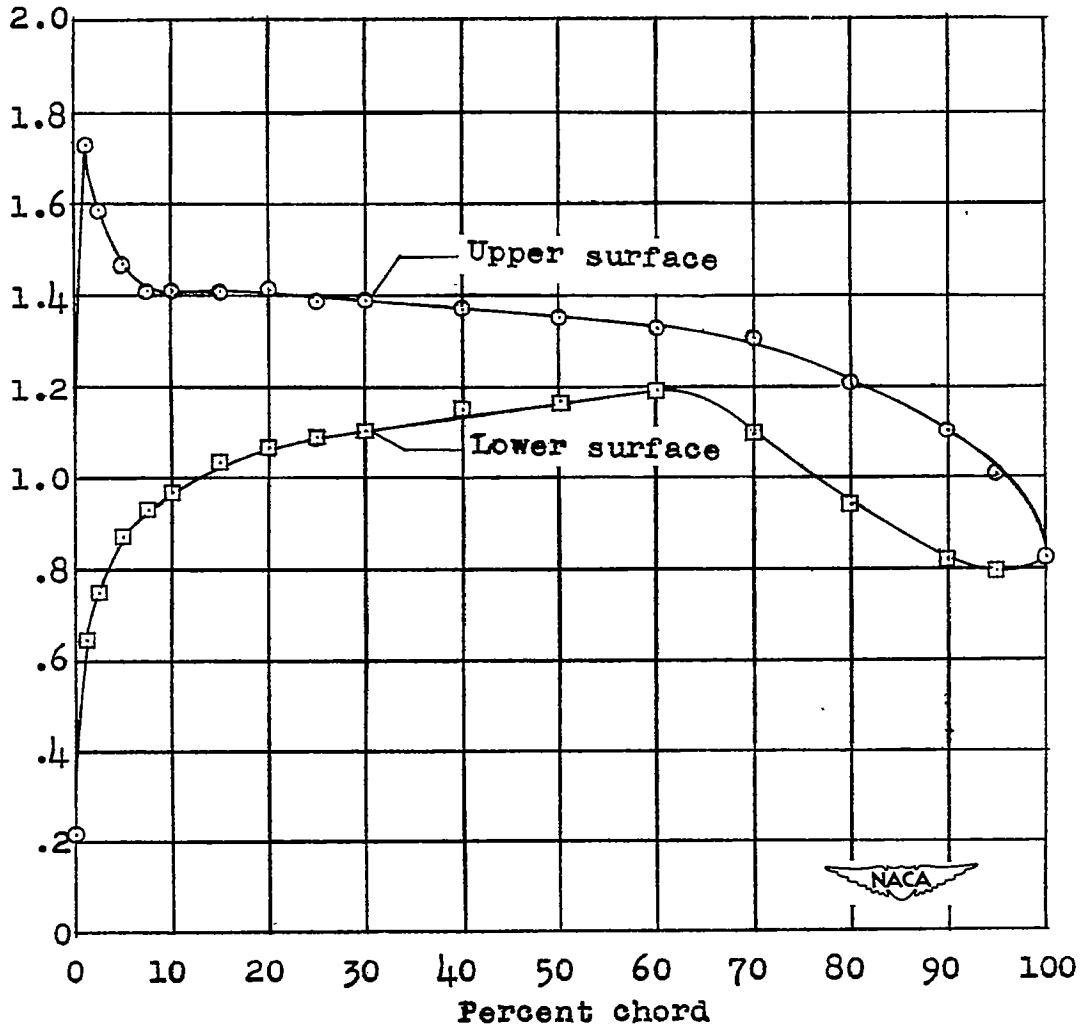


(n) $\alpha_o = 1.5^\circ$; $c_l = 0.30$.

Figure 6.- Continued.

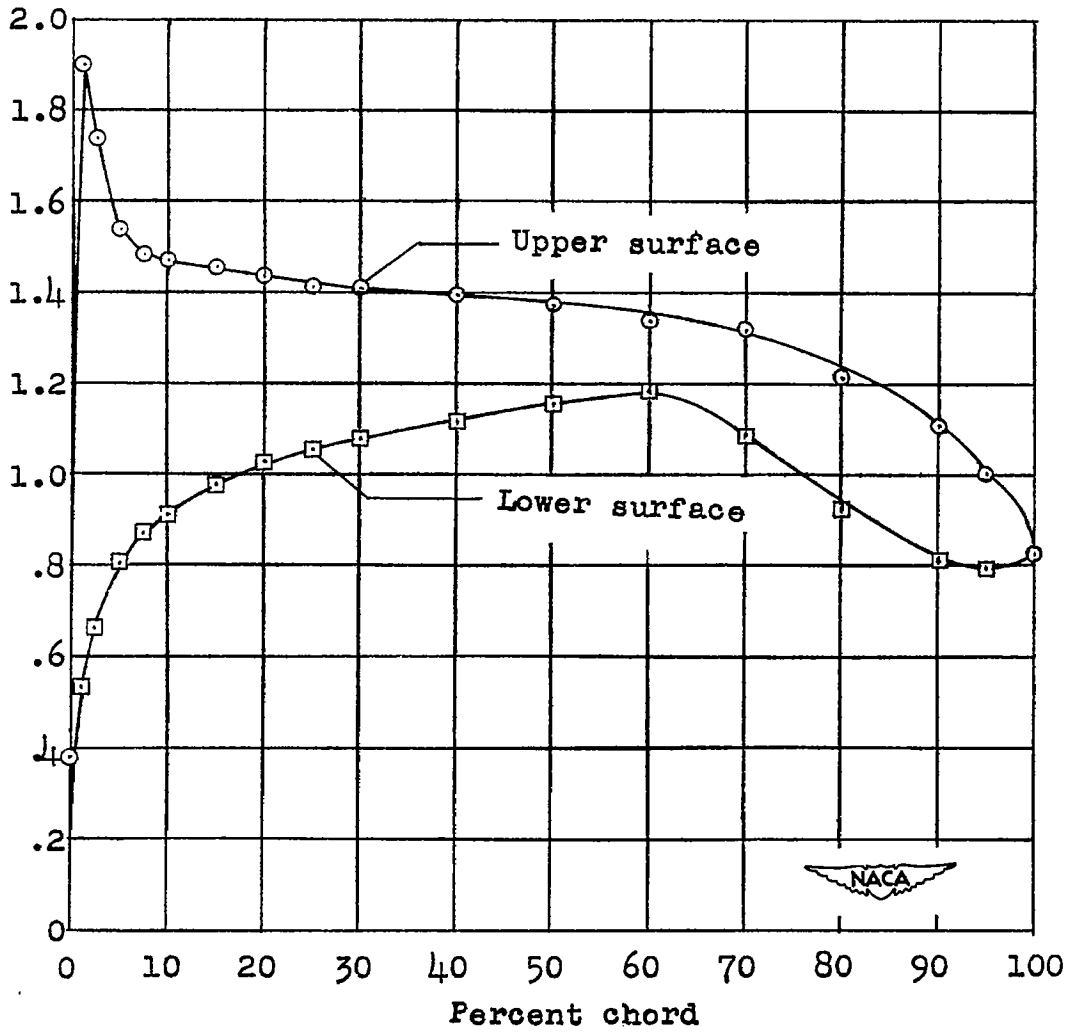


(o) $\alpha_o = 2.0^\circ$; $c_l = 0.37$.

Figure 6.- Continued.

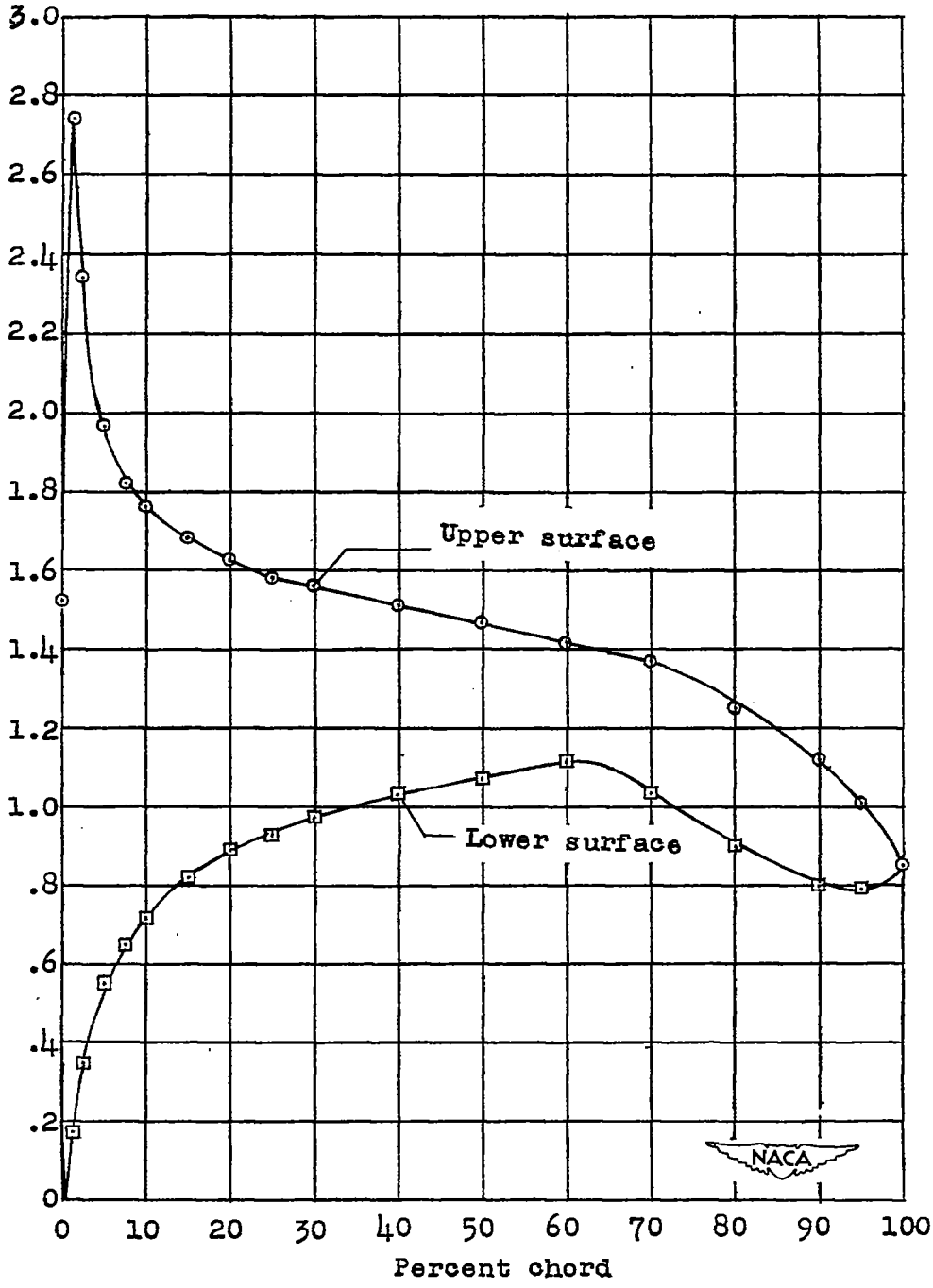


(p) $\alpha_o = 4.0^\circ$; $c_l = 0.58$.

Figure 6.- Continued.

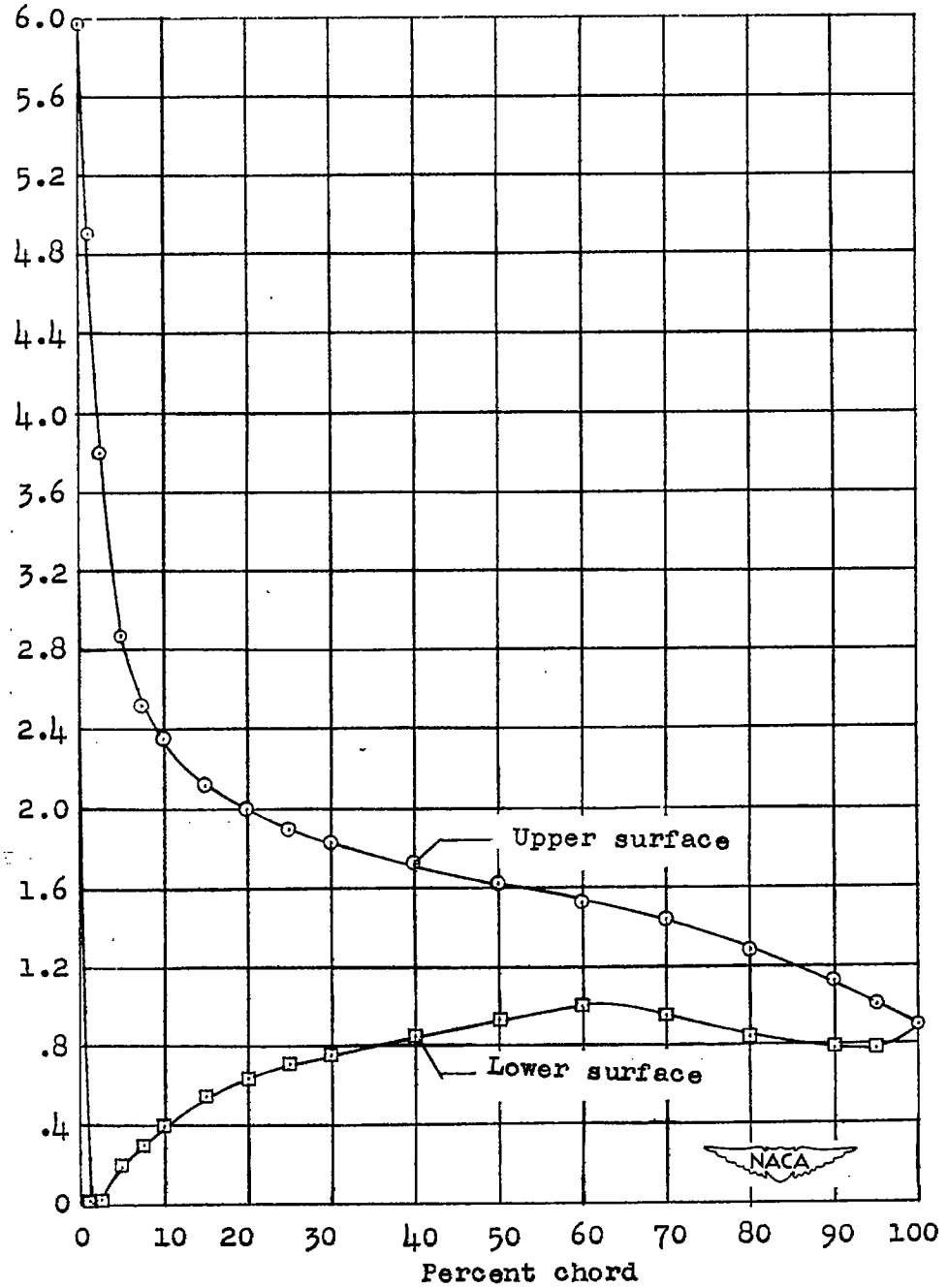


(q) $\alpha_o = 8.0^\circ$; $c_l = 0.99$.

Figure 6.- Continued.

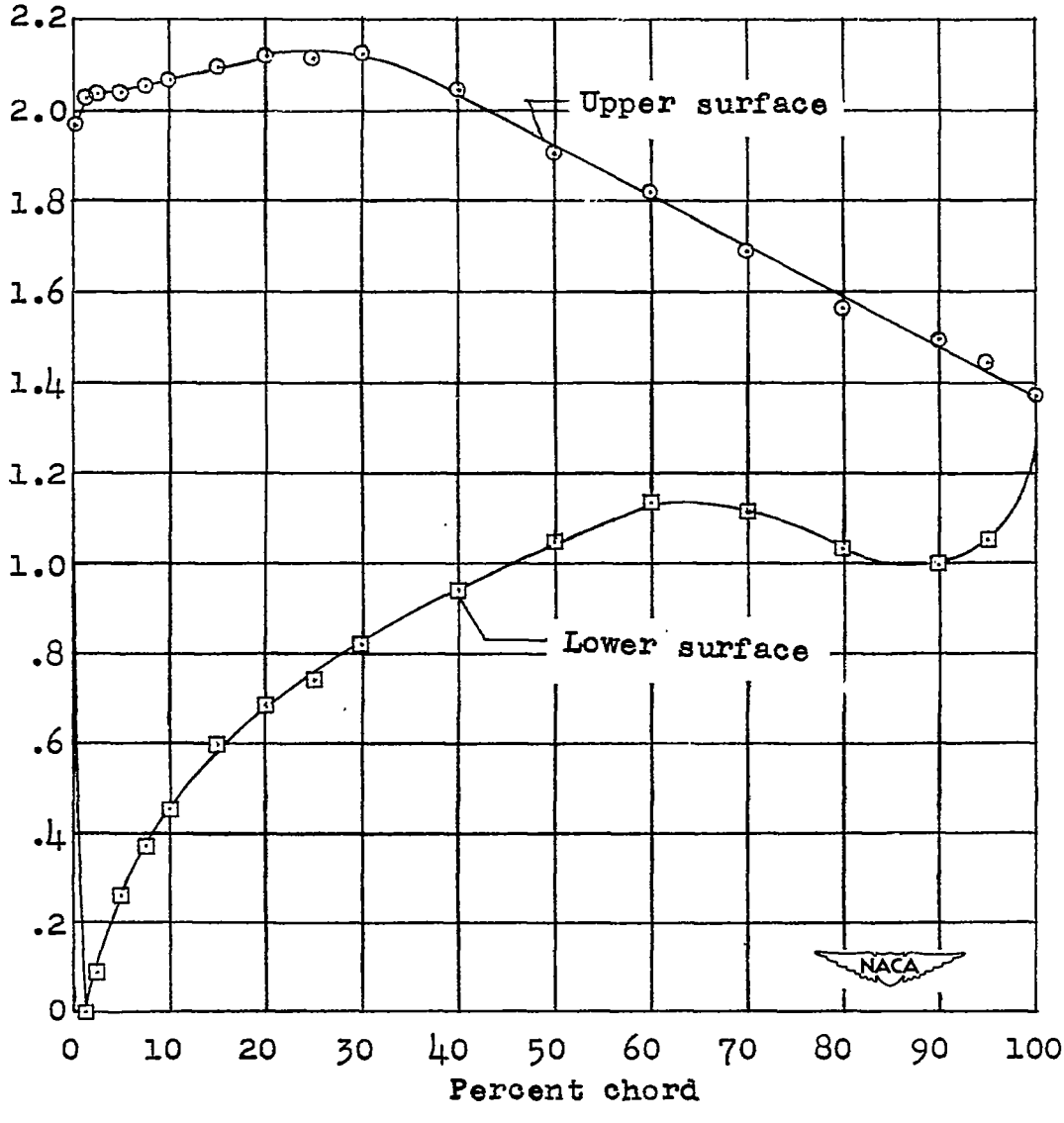


(r) $\alpha_o = 12.0^\circ$; $c_l = 1.24$.

Figure 6.- Concluded.

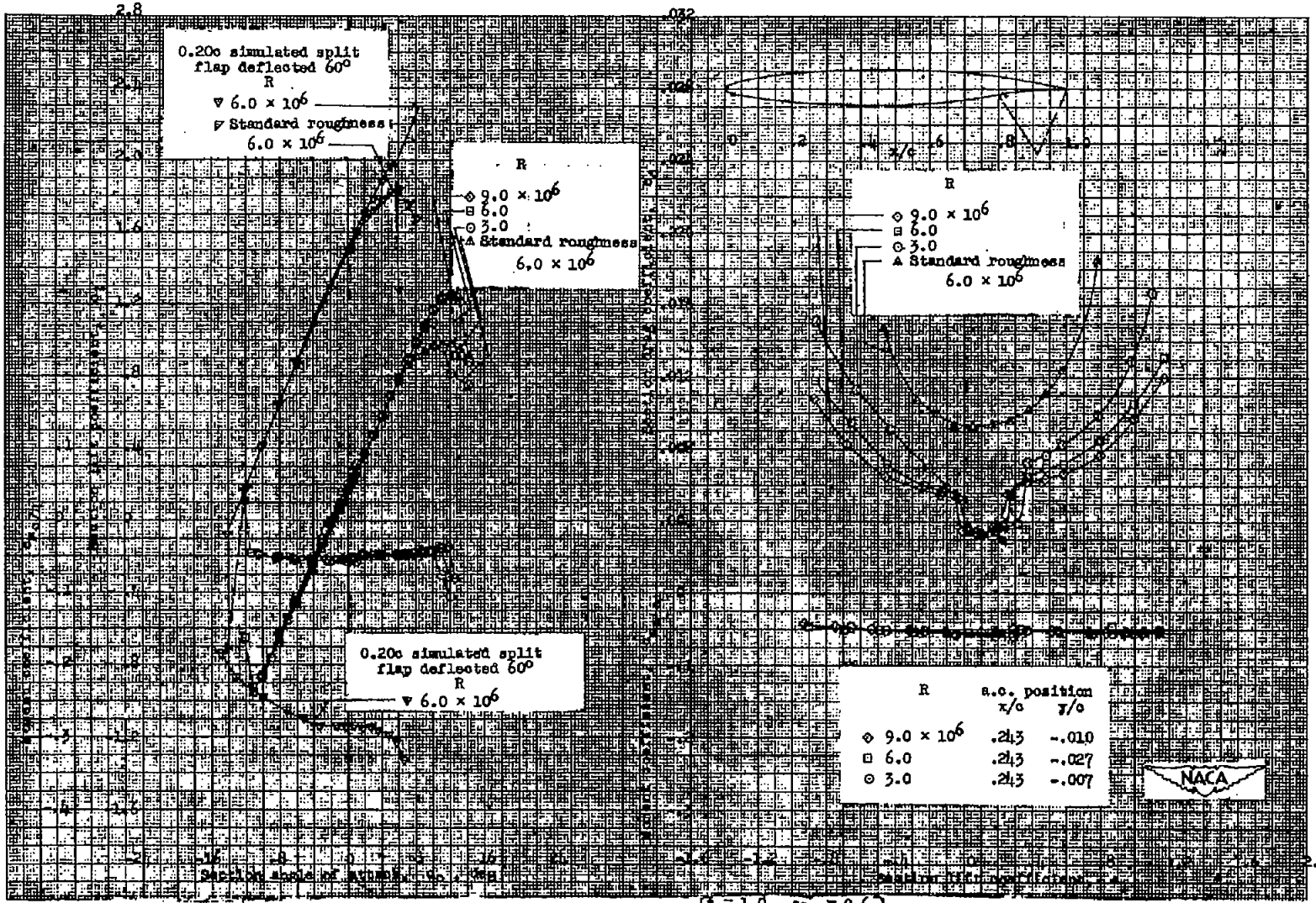


Figure 7.- Aerodynamic characteristics of the NACA 66(09)-210 $\begin{Bmatrix} a = 1.0, & c_{l_i} = 0.6 \\ a = 0.6, & c_{l_i} = -0.4 \end{Bmatrix}$ airfoil section, 24-inch chord.

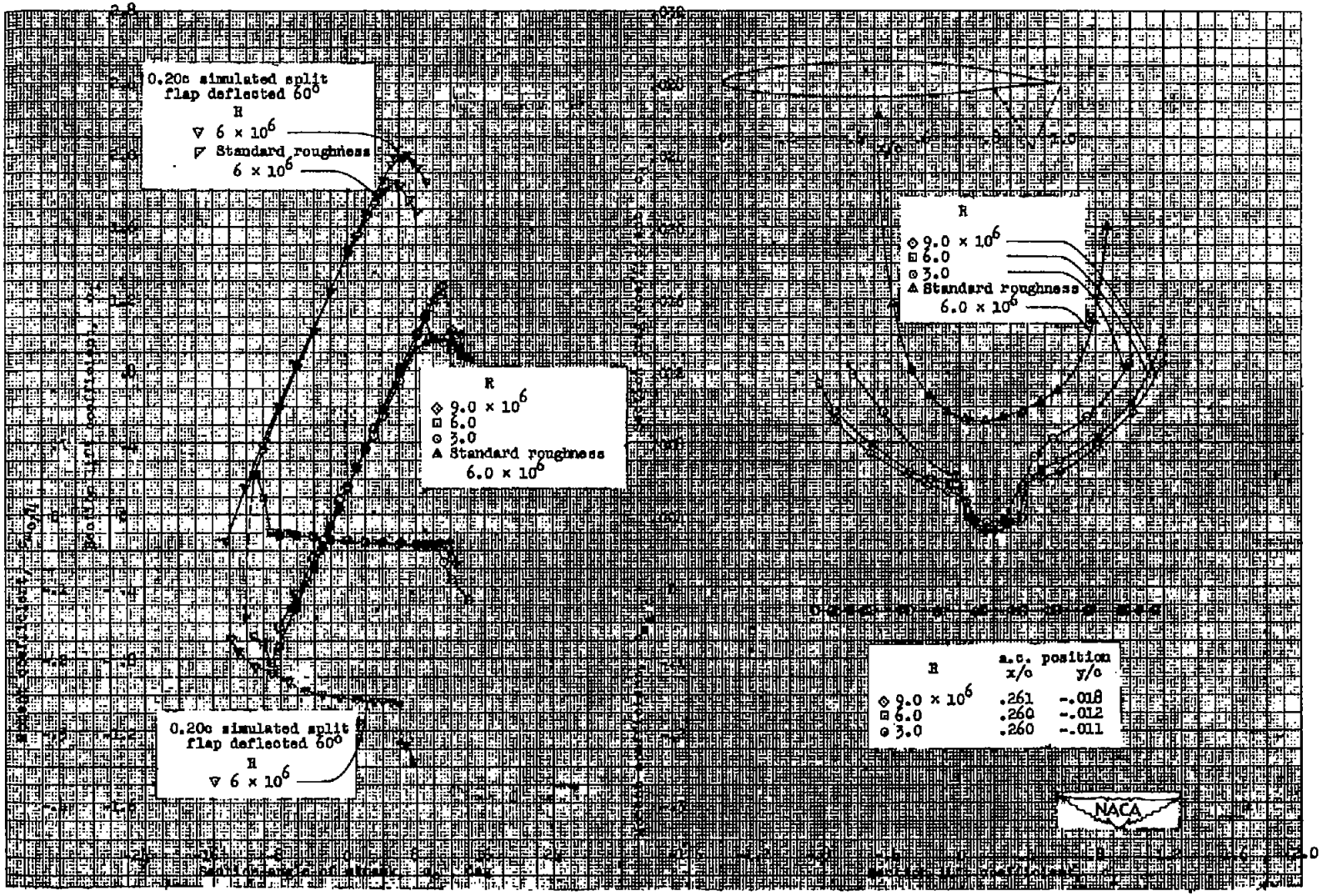


Figure 8.- Aerodynamic characteristics of the NACA 66-210 airfoil section, 24-inch chord.